

Anisotropies of Diffusive Ultra-high Energy Cosmic Rays in $f(R)$ Gravity Theory

Swaraj Pratim Sarmah^{*} and Umananda Dev Goswami[†]

Department of Physics, Dibrugarh University, Dibrugarh 786004, Assam, India

Understanding the anisotropy of ultra high-energy cosmic rays (UHECRs) is crucial for unraveling the origins and propagation mechanisms of these enigmatic particles. In this work, we studied the dipolar anisotropy of UHECRs in the diffusive regime by considering three cosmological models: the standard Λ CDM model, $f(R)$ gravity power-law model and the Starobinsky model. This work aims to see the role of the $f(R)$ gravity theory in understanding the anisotropy of UHECRs without condoning the standard cosmology. We found that the amplitude of the dipolar anisotropy is sensitive to these cosmological models, with the $f(R)$ power-law model predicting the largest amplitude, while the Λ CDM model predicting the smallest amplitude at most of the energies in the range considered. The predicted amplitude of the Starobinsky model lies within the range of the Λ CDM one. This work not only provides a way for exploration of UHECRs anisotropy within different cosmological contexts but also may pave the way for new avenues of research at the intersection of high-energy astrophysics.

Keywords: Ultra High Energy Cosmic Rays; Anisotropies, $f(R)$ gravity

I. INTRODUCTION

Although it is thought that cosmic rays (CRs) are mostly of galactic origin below 10^{17} eV and are most likely related to supernova remnants or pulsars [1–3], their sources are still unknown. At ultra-high energies (UHEs) ($\geq 10^{18}$ eV), CRs are most likely extragalactic in origin [4]. The main support for this theory comes from the fact that at energies of a few EeV ($1 \text{ EeV} = 10^{18}$ eV), where the chemical composition is comparatively of low mass nuclei [5], the galactic magnetic field is not strong enough to cause CRs to diffuse within the galaxy and the arrival directions do not exhibit any noticeable correlation to the distribution of galactic matter [6, 7]. Also, their extragalactic origin is supported by the detection of a dipolar distribution in the arrival directions of the CRs with energies above 8 EeV, which points away from the Galactic center direction [8]. The primary factors that help us to understand the properties of CRs are their energy spectrum, and anisotropies in their arrival directions which are measured at various angular scales. The changes in the slope of the spectrum can indicate alterations in propagation mechanisms or shifts in the source population, like the dominance of the extragalactic component above the ankle. These changes can also occur at intermediate energies. Additionally, the impact of energy losses due to pair production on extragalactic protons interacting with the cosmic microwave background (CMB) [9–11], or diffusion effects [12], can contribute to shaping the CR spectrum at energies in the EeV range. There are some key features in the UHECR spectrum: a slight increase in the intensity of the spectrum at the ankle around 5 EeV, then a softening of the spectrum at ~ 13 EeV [13, 14], followed by a significant drop starting at approximately 50 EeV [15, 16].

Because of the incredibly high energies of CR's particles, they surpass the energy that human-made accelerators can achieve. However, their arrival rate on Earth is meager, with only about one particle reaching the atmosphere per square kilometer per century with energies around or above 6×10^{19} eV. Physicists are working hard to improve the accuracy and exposure to this tiny flux in order to unravel the mystery of these particles and their origins. Recent experimental advancements have been significant in this pursuit. One important discovery is that there is a decrease in the flux of CRs above 4×10^{19} eV compared to what was expected based on lower energy observations. This suppression has been confirmed by multiple studies [13, 17–19]. The observed suppression in the flux above 4×10^{19} eV could be due to the loss of energy during propagation over vast cosmological distances, a phenomenon predicted nearly fifty years ago [20, 21]. However, the current data is insufficient to determine if energy loss is the sole cause for this suppression. Researchers have also set upper limits on the presence of photons [22–24], neutrinos [25–27], and neutrons [28] among the UHECRs. Evidence from the Pierre Auger Observatory (PAO) suggests a shift from a lighter to a heavier composition as the energy of CRs increases beyond $\sim 3 \times 10^{18}$ eV [29–32].

Physicists are still unsure about where UHECRs come from. However, they believe that by studying the anisotropies in their arrival directions, they may eventually figure it out [33–35]. The challenge in this direction is that CRs, which are charged particles, are deflected by magnetic fields from their source directions in galactic or extragalactic spaces. Thus their arrival directions do not necessarily point to their sources. But as the rays gain more momentum, their deflection becomes less significant, especially towards the end of the highest energies observed. This gives hope that we can find the closest powerful sources outside our galaxy by looking for clusters of UHECRs pointing towards them. There are various possible types of extragalactic sources

* Email: swarajpratimsarmah16@gmail.com

† Email: umananda2@gmail.com

of UHECRs. The traditional viewpoint suggests that these sources could include powerful objects like gamma-ray bursts, tidal disruption events, active galactic nuclei, and galaxy mergers. It is important to consider how the brightness of these sources changes with distance (measured by redshift) because it affects both the weakening of CRs intensity at the highest energies and the creation of secondary particles through interactions with cosmic radiation backgrounds. These interactions can produce fragments from heavier CR particles or generate photons and neutrinos through photo-pion interactions. These studies have been conducted to investigate the importance of nearby sources in explaining the CR spectrum at extremely high energies. Additionally, it has been examined how these nearby sources may contribute to the observed patterns of anisotropy at intermediate angular scales. The PAO has observed the patterns of large-scale anisotropy in CR arrival directions. These patterns are naturally linked to the uneven distribution of galaxies in our nearby region, within a few hundred Mpc [36]. Researchers have investigated the significance of nearby sources in explaining the spectrum of CRs at extremely high energies, as well as their potential role in accounting for anisotropies observed on intermediate angular scales [37–40]. The UHECRs detected by PAO on a large angular scale, analysed over three orders of magnitude in energy [41]. For more than 4 EeV, the dipolar amplitude increases with energy [36]. Also, the researchers at the PAO have analyzed the arrival directions of more than 2600 UHECRs above 32 EeV, providing evidence for a deviation from isotropy at an intermediate angular scale with a 4σ confidence level for UHECR energies above 40 EeV [42]. The isotropy of UHECRs is disfavoured with 4σ confidence level in PAO observation with starburst galaxies, which is one of the significant results in UHECRs anisotropy [43]. The same kind of results can also be found in other giant CR experiments like Telescope Array [44–47]. In addition to studying the distribution of arrival directions of CRs with energy, it also needs to understand how the composition of CRs changes with energy. Separating lighter and heavier components, which experience different levels of deflection, could also provide useful information and scientists are currently upgrading the Pierre Auger Observatory to help with these investigations.

The General Relativity (GR) developed by Albert Einstein in 1915 to explain gravitational interactions can be considered as the most beautiful, well-tested, and successful theory in this area. In 2015, the LIGO detectors [48] detected the Gravitational Waves (GWs), which were predicted by Einstein almost a century earlier from his theory of GR. Additionally, in 2019, the Event Horizon Telescope [49–54] released the first image of a supermassive black hole in the galaxy M87. These discoveries provide robust support for GR. However, GR has been suffering from some serious drawbacks also, such as the lack of a complete quantum theory and its inability to explain the current accelerated expansion of the Universe [55–58] as well as the missing mass [59–63] in galaxies’ rotational dynamics. To address these issues, Modified Theories of Gravity (MTGs) have been developed along with the concept of dark energy [64, 65]. One widely used MTG is the $f(R)$ theory of gravity [66], where the Ricci scalar R in the Einstein-Hilbert action is replaced by a function $f(R)$. In recent times various models of $f(R)$ gravity, i.e. the functional forms of $f(R)$ have been proposed to explain these cosmic phenomena. Some of extensively used and viable models of $f(R)$ gravity are the Starobinsky model [67, 68], Hu-Sawicki model [69], power-law model [70, 71], and Tsujikawa model [72].

Various research groups have used various methods to study CR anisotropy and propagation till now [4, 73–82]. Considering the significant contributions of MTGs in understanding cosmological [83, 84] and astrophysical [85–88] issues in recent times, it is prudent to explore the application of MTGs in the field of CRs to address the current challenges in this domain. With this motivation, in this work, we are interested in studying CR anisotropies in the energy range between 10^{17} eV and 10^{20} eV in the realm of MTGs for the very first time. In our previous work, we studied flux and propagation properties of UHECRs in the $f(R)$ theory of gravity [89]. In that study, we here considered two very well-known $f(R)$ gravity models, viz., the power-law model [70] and the Starobinsky model [68]. In this study also we use these two models of $f(R)$ gravity along with the standard Λ CDM model for comparison. The chief aim of our study is to see the effect of $f(R)$ gravity theory on the anisotropic behaviour of UHECRs in comparison to the standard cosmological perspective, rather than justifying the correctness of theory in terms of observational data of this interesting behaviour of CRs.

The rest of the parts of this paper are arranged as follows. Since in this study, we consider the $f(R)$ gravity theory as the basic cosmological theory required to study the propagation of UHECRs in galactic and extragalactic spaces, in Section II we discuss briefly the $f(R)$ gravity models used in this study and also present the required cosmological equations obtained for those models. Section III is divided into two parts. Subsection III A is dedicated for the theoretical formalisms of the propagation of UHECRs in turbulent magnetic fields (TMF) and hence their consequent dipolar anisotropy. The numerical calculations of the anisotropies of UHECR protons along with a few nuclei have been analysed and discussed in Subsection III B. Finally, we summarize our results and give final remarks in Section IV.

II. $f(R)$ GRAVITY MODELS AND COSMOLOGICAL EQUATIONS

In this study, we use two most prevalent and viable $f(R)$ gravity models: the power-law model and the Starobinsky model. It should be mentioned at this point that two $f(R)$ models are used to gain confidence in the obtained results from the comparison and also to understand their performance in this sector of CR physics. Here we briefly introduce these two models and also write the expressions of the Hubble parameter $H(z)$ for them. These expressions of $H(z)$ will be used to calculate different parameters for both models. The details about these two models and derivations of the expressions of $H(z)$ for them can be

obtained in Refs. [68, 70, 71, 89].

The functional form of the power-law model is given by [70, 71]

$$f(R) = \sigma R^n, \quad (1)$$

where σ and n are two free model parameters. The best-fitted value of the model parameter n is found as 1.4 [70]. The parameter σ relies on H_0 , n and Ω_{m0} as given by

$$\sigma = -\frac{3H_0^2 \Omega_{m0}}{(n-2)R_0^n}. \quad (2)$$

The expression of the Hubble parameter $H(z)$ for this model can be written as [70]

$$H(z) = \left[-\frac{2nR_0}{3(3-n)^2 \Omega_{m0}} \left\{ (n-3)\Omega_{m0}(1+z)^{\frac{3}{n}} + 2(n-2)\Omega_{r0}(1+z)^{\frac{n+3}{n}} \right\} \right]^{\frac{1}{2}}, \quad (3)$$

where R_0 is the present value of the Ricci scalar and is given by [70]

$$R_0 = -\frac{3(3-n)^2 H_0^2 \Omega_{m0}}{2n[(n-3)\Omega_{m0} + 2(n-2)\Omega_{r0}]}. \quad (4)$$

Our study aims to elucidate the correlation between the redshift of a remote celestial entity and its age. This objective can be achieved through an exploration of the relationship between redshift and the evolution of cosmological time, which is given by

$$\left| \frac{dt}{dz} \right| = \frac{1}{(1+z)H(z)}. \quad (5)$$

Using Eq. (3), we can write Eq. (5) for the power-law model as

$$\left| \frac{dt}{dz} \right| = (1+z)^{-1} \left[-\frac{2nR_0}{3(3-n)^2 \Omega_{m0}} \left\{ (n-3)\Omega_{m0}(1+z)^{\frac{3}{n}} + 2(n-2)\Omega_{r0}(1+z)^{\frac{n+3}{n}} \right\} \right]^{-\frac{1}{2}}. \quad (6)$$

Again for the Starobinsky model, we consider the functional form as [68]

$$f(R) = \alpha R + \beta R^2. \quad (7)$$

Here α and β are two model parameters. The best-fitted values of these model parameters are found to be 1.07 and 0.00086, respectively [89]. The expression for the Hubble parameter for the Starobinsky model can be obtained as [89]

$$H(z) = H_0 \left[\frac{3\Omega_{m0}(1+z)^3 + 6\Omega_{r0}(1+z)^4 + (\alpha R + \beta R^2)H_0^{-2}}{6(\alpha + 2\beta R) \left\{ 1 - \frac{9\beta H_0^2 \Omega_{m0}(1+z)^3}{\alpha(\alpha + 2\beta R)} \right\}^2} \right]^{\frac{1}{2}}. \quad (8)$$

And thus using the above expression of $H(z)$, we can write the Eq. (5) explicitly for the Starobinsky model as

$$\left| \frac{dt}{dz} \right| = [(1+z)H_0]^{-1} \left[\frac{3\Omega_{m0}(1+z)^3 + 6\Omega_{r0}(1+z)^4 + \frac{\alpha R + \beta R^2}{H_0^2}}{6(\alpha + 2\beta R) \left\{ 1 - \frac{9\beta H_0^2 \Omega_{m0}(1+z)^3}{\alpha(\alpha + 2\beta R)} \right\}^2} \right]^{-\frac{1}{2}}, \quad (9)$$

The expressions of $|dt/dz|$ for both the cosmological models can be used to calculate the density enhancement factor, modification factor, CR flux etc., which are discussed in detail in Ref. [89]. We use the Hubble constant $H_0 \approx 67.4 \text{ kms}^{-1} \text{ Mpc}^{-1}$ [90], matter density parameter $\Omega_{m0} \approx 0.315$ [90] and radiation density parameter $\Omega_{r0} \approx 5.373 \times 10^{-5}$ [91] in our numerical calculations.

III. ANISOTROPY OF ULTRA-HIGH ENERGY COSMIC RAYS

In this section, we delve into the exploration of UHECRs' anisotropy in the light of two models of $f(R)$ theory of gravity, the power-law model and the Starobinsky model as mentioned in the previous section, considering the propagation of UHECRs in the presence of TMFs. This section is bifurcated into two subsections for a systematic detailed analysis. The theoretical formalism for examining the anisotropy of UHECRs in the presence of a TMF in the $f(R)$ theory of gravity is developed in the first subsection. The second subsection is devoted to the numerical analysis of the obtained theoretical formulation and to the related discussions.

A. Theoretical Formalism

It is believed that the evolution of primordial seeds ~ 1 nG impacted by the process of structure building may generate the TMFs in the Universe at present [92, 93]. Magnetic fields with some strength associated with matter density are often augmented in dense places, such as superclusters. Extragalactic magnetic fields can also be produced by galactic outflows, in which galactic magnetic fields are transported into the intra-cluster medium by winds. Although magnetic fields with μG strengths have been recorded in cluster cores, they are projected to be smaller at supercluster scales, and values ranging from 1 nG to 100 nG have been studied [94–96], with the assumed coherence length l_c of the order of 0.1 – 1 Mpc [97]. We will consider the individual CR sources in the local supercluster, which is a group of galaxies that includes our own Milky Way galaxy. The local supercluster is located within 100 Mpc of Earth. For simplicity, we will assume that a uniform, isotropic TMF is present within the diffusion region, which is the region of space where CRs can propagate. The field will be characterized by a root mean square strength $B = \sqrt{\langle B^2(x) \rangle}$. An effective Larmor radius for charged particles can be defined as

$$r_L = \frac{E}{ZeB} \simeq 1.1 \frac{E/\text{EeV}}{ZB/\text{nG}} \text{ Mpc}. \quad (10)$$

The Larmor radius is equal to the coherence length at the critical energy E_c , which distinguishes between resonant diffusion at low energies and non-resonant diffusion at high energies, i.e. $l_c = r_L(E_c)$. The critical energy of the particles is a significant factor in the study of the diffusion of charged particles in magnetic fields and it is given by

$$E_c = ZeBl_c \simeq 0.9Z \frac{B}{\text{nG}} \frac{l_c}{\text{Mpc}} \text{ EeV}. \quad (11)$$

The critical energy E_c distinguishes between two regimes of CRs diffusion, resonant diffusion at low energies ($< E_c$) and non-resonant diffusion at high energies ($> E_c$). In the resonant diffusion regime, CRs are deflected by magnetic field fluctuations with scales comparable to the Larmor radius. In the non-resonant diffusion regime, deflections are smaller and can only occur over distances greater than l_c . The diffusion coefficient D as a function of energy is given by [4]

$$D(E) \simeq \frac{cl_c}{3} \left[4 \left(\frac{E}{E_c} \right)^2 + a_I \left(\frac{E}{E_c} \right) + a_L \left(\frac{E}{E_c} \right)^{2-m} \right], \quad (12)$$

where c is the speed of light. In the case of the Kolmogorov spectrum $m = 5/3$, $a_L \approx 0.23$ and $a_I \approx 0.9$, and for that of Kraichnan spectrum $m = 3/2$, $a_L \approx 0.42$ and $a_I \approx 0.65$. The density ρ of relativistic particles propagating from a source that lies at \mathbf{x}_s in an expanding Universe obeys the equation during the diffusion phase as [98]

$$\frac{\partial \rho}{\partial t} + 3H(t)\rho - b(E, t) \frac{\partial \rho}{\partial E} - \rho \frac{\partial \rho}{\partial E} - \frac{D(E, t)}{a^2(t)} \nabla^2 \rho = \frac{Q_s(E, t)}{a^3(t)} \delta^3(\mathbf{x} - \mathbf{x}_s), \quad (13)$$

where $H(t) = \dot{a}(t)/a(t)$ is the Hubble parameter, $a(t)$ is the scale factor, \mathbf{x} describes the comoving coordinates, $Q_s(E)$ is a source function which denotes the number of particles that are emitted with energy E per unit time. The energy losses of the emitted particles are described by

$$\frac{dE}{dt} = -b(E, t), \quad b(E, t) = H(t)E + b_{int}(E). \quad (14)$$

This comprises energy redshift due to cosmic expansion and energy losses due to interactions with radiation backgrounds, including pair production and photo-pion generation as a result of interactions with the CMB (for details see [4]). For the case of zero energy losses, the solution of Eq. (13) is given by

$$\rho(r_s, t, E) = \frac{Q(E) \exp[-r_s^2/4Dt]}{(4\pi Dt)^{3/2}}, \quad (15)$$

where r_s is the source distance. Now, integrating this Eq. (15) over time, we obtain the solution as

$$\rho(r_s, E) = \frac{Q(E)}{4\pi r_s D(E)}. \quad (16)$$

The general solution of Eq. (13) including the energy losses have been taken into account was given by [98] as

$$\rho(E, r_s) = \int_0^{z_i} dz \left| \frac{dt}{dz} \right| Q(E_g, z) \frac{\exp[-r_s^2/4\lambda^2]}{(4\pi\lambda^2)^{3/2}} \frac{dE_g}{dE}, \quad (17)$$

where z_i is the initial redshift and E_g is the generation energy having energy E at the redshift $z = 0$. The parameter dt/dz is the relation between cosmological time evolution and the redshift as we have already discussed in Section II. λ is the Syrovatsky variable [99, 100] and it is given as

$$\lambda^2(E, z) = \int_0^z dz \left| \frac{dt}{dz} \right| (1+z)^2 D(E_g, z). \quad (18)$$

The variable $\lambda(E, z)$ represents the conventional distance covered by CRs originating at redshift z with energy E_g , from their point of generation to the current moment when their energy has decreased to E . We are interested in the expression that quantifies the rate at which the energy of particles at their source degrades about their energy at $z = 0$, denoted as dE_g/dE and is given by [11, 98]

$$\frac{dE_g}{dE} = (1+z) \exp \left[\int_0^z dz \left| \frac{dt}{dz} \right| \left(\frac{\partial b_{int}}{\partial E} \right) \right]. \quad (19)$$

The detailed derivation of dE_g/dE was nicely performed by Berezhinsky et al. in Appendix B of Ref. [11]. In the following we will implement the power-law and Starobinsky models' results from Ref. [89] to obtain the CR's protons density enhancement factor, and subsequently the CR's protons flux and finally the CR anisotropies as predicted by these two $f(R)$ gravity models. We calculate the dipolar anisotropy using Ref. [101] as

$$\Delta = 3 \frac{\eta}{\xi}, \quad (20)$$

which is identical to the expression in Ref. [4] (according to [101]). Here, η and ξ are the modification factor and enhancement factor respectively. The analytical expressions for η and ξ are taken from Refs. [74, 89] and accordingly we will proceed to calculate it for the Λ CDM model, power-law model and the Starobinsky model. It needs to be mentioned that at sufficiently high energies, CR enters the quasi-rectilinear regime, where only angular diffusion occurs but there is no role of the spatial diffusion. In our work, the considered anisotropy Eq. (20) which depends on the modification factor and enhancement factor is valid for a wide range of energies (see Ref. [101]). The reason for choosing this model is that it is compatible with different cosmological models. Although the quasi-rectilinear regime is certainly important and relevant at sufficiently high energies, it falls outside the scope of our current study. Further, the Λ CDM model is used here as a standard model for comparison with the $f(R)$ gravity models' results.

It would be pertinent to mention at this point that the dipolar anisotropy of UHECRs is influenced by the distribution of their sources and their propagation behaviours in the intergalactic medium. The propagation behaviours are determined by the cosmological parameters, which differ in different cosmological models. Each of these models has a different set of cosmological parameters, which leads to different propagation effects and hence different predictions for the dipolar anisotropy. To present this point clearly, we show the plots of $H(z)$ and dt/dz with respect to z for all three considered models in Fig. 1. One can see from these plots that both $f(R)$ gravity models along with the Λ CDM model satisfy the available $H(z)$ observational data. This demonstrates that these $f(R)$ gravity models are consistent with observations, despite the differences in their predictions of $H(z)$ values at different z . It is seen that there are overlappings of all three models at $z \sim 0.029$ and 2.8 within the considered range of z . Whereas, except around these overlapping points there is a noticeable difference in the predictions of the power-law model from the other two models. Power-law model predicts lower values of dt/dz (higher values of $H(z)$) than that for the other two models from $z \sim 0.029$ to $z \sim 2.8$. For $z \gtrsim 2.8$ the power-law model predicts higher values of dt/dz .

B. Numerical Results and Discussions

Using Eq. (20) we calculate the anisotropies of UHECRs for the considered $f(R)$ gravity models: the power-law model and the Starobinsky model, at selected source distances of 30, 60, and 90 Mpc considering the composition of UHECRs as pure proton for simplicity. The same calculations are also done for the standard Λ CDM model for the comparative analysis. The results of these calculations are shown as contour plots in Fig. 2. For the calculation purpose, unless specified otherwise, we take the coherence length $l_c = 0.25$ Mpc. This considered coherence length lies within its range of values used in the literature as mentioned earlier. It is to be noted that the enhancement factor ξ is directly proportional to l_c . So increasing l_c leads to an increase in the enhancement factor, hence decreasing the anisotropy. The contours show the levels of anisotropy at different energy and magnetic field values. The color scale in each plot represents the level of anisotropy, from high at the top to low at the bottom. It is seen that for a given magnetic field, the CR anisotropy increases as the energy increases, which is an established fact. This is because the deflection of CRs by the galactic magnetic field decrease with increasing energy. At low energies, the deflections are large enough to randomize the arrival directions of the CRs, making them appear isotropic. On the other hand, at high energies, the deflections are small enough that the CRs can still retain some of their directional information. This leads to an increase in the anisotropy at high energies.

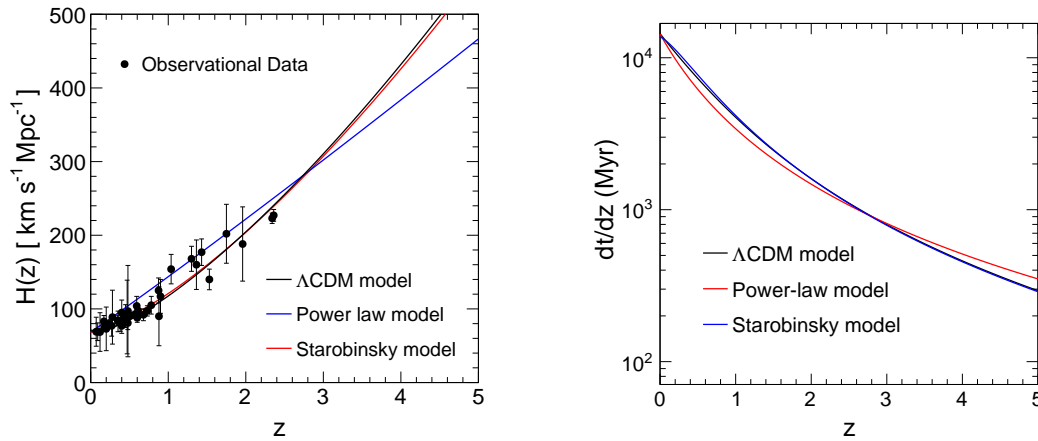


FIG. 1. Hubble parameter $H(z)$ with the observational Hubble dataset (left panel) and dt/dz (right panel) as a function of the redshift z for the Λ CDM, power-law and the Starobinsky model.

The results of the plots show that the CRs' anisotropy is strongly dependent on both energy and magnetic field. At high energies and less strength of the magnetic field, the anisotropy is very high, with a level of about 0.02 to 1.4 depending on the cosmological model as well as the source distance considered. This means that CRs of high energies in a low magnetic field region are much more likely to come from a particular direction than CRs of low energies in a region of a high magnetic field. In contrast, at high energies and higher strength of the magnetic field, the anisotropy is quite low, with a level of about 0.03 to 0.48 depending on the considered model and the source distance. This means that CRs even at high energies with the effect of stronger magnetic fields are much more isotropic, or evenly distributed in all directions. These results of the plots can be explained from the process of diffusion of CRs in the galactic or extragalactic magnetic field. As mentioned already, it is obvious that at low energies, CRs are more easily scattered by the magnetic field, which reduces their anisotropy. But other factors such as source distance and strength of magnetic field also have effects on their anisotropy simultaneously. At high energies, CRs are not easily scattered by the magnetic field, which allows them to travel in straighter lines and maintain their anisotropy. However, a much stronger magnetic field can scatter even UHECRs sufficiently to have isotropic distribution as indicated by the plots. We also draw the contour plots for different source distances in Fig. 2. It is seen that as the distance from the sources increases, the anisotropy of CRs decreases. As a whole, the Λ CDM model shows the least anisotropies among others, while the $f(R)$ power-law model shows much higher values of anisotropy. The Starobinsky model shows the anisotropy values within the Λ CDM model and the power-law model. Thus the $f(R)$ gravity models give the anisotropy values that are in a wider range than that of the Λ CDM model.

To specify some of the points clearly as discussed above with some additional features, we draw the UHECRs' anisotropy with respect to energy, source distance, and strength of the magnetic field in Fig. 3. Each plot of the figure is obtained by keeping any two fixed at their specific values while taking one as a variable from energy, source distance, and magnetic field strength. The different curves in the plots of the figure represent different cosmological models. It is to be noted that the Λ CDM is the model that is most commonly used in CR studies. As mentioned earlier the $f(R)$ power-law model and the Starobinsky model are the models that we propose to study the behaviour of anisotropy of UHECRs. From the figure, we see that at a given source distance and the magnetic field value (see top plots), the power-law model depicts the highest values of anisotropy for the whole range of energies considered (within the UHE scale). While the Λ CDM model depicts the lowest anisotropy values for the whole energy range, especially at a small source distance. However, at a long source distance, the Starobinsky model predicts the lowest anisotropy in the lower energy range. For example at $r_s = 40$ Mpc, the Starobinsky model gives the lowest anisotropy values for energies $E < 0.3$ EeV. This range of energy may become wider by shifting towards the higher energy side for more strong magnetic fields. Only above this energy range, the Λ CDM model depicts the lowest values in this case. Moreover, in the lower energy range, the Λ CDM model and the Starobinsky model depict the same anisotropy value at a particular energy depending on the source distance and magnetic field strength. As an example, for $r_s = 40$ Mpc and $B = 20$ nG, the same anisotropy value is predicted by these two models at ~ 0.3 EeV. The middle panels show the variation of anisotropy of UHECRs with the source distance for the two sets of fixed values of energy and magnetic field strength. Here the anisotropy decreases with increasing the source distance as expected and the power-law model predicts maximum anisotropy values throughout the considered range of source distances. Lastly, the bottom panels show the behaviour of anisotropy of UHECRs with the magnetic field strength for the two sets of fixed values of energy and source distance. As anticipated it is seen that anisotropy decreases with an increase in magnetic field strength. It is also seen from here that anisotropy increases with an increase in energy as observed earlier. In this case also the power-law model gives the highest anisotropies followed by the Starobinsky model and Λ CDM model.

Nevertheless, it is to be noted that the difference in prediction of anisotropy by these cosmological models decreases with an increase in both source distance and the magnetic field strength. This is due to the reason that as the anisotropy decreases with increasing source distance and the magnetic field strength, the difference of prediction of anisotropy by cosmological models also decreases.

Still, to lucidly visualise the effect of the cosmological models on the UHECRs' anisotropy, we plot the anisotropy with respect to energy from 1 EeV to 100 EeV considering a small source distance $r_s = 10$ Mpc and a very weak magnetic field $B = 1$ nG on the left panel of Fig. 4 for all three cosmological models considered. From this plot, one can see that even in this scenario also there is a considerable effect of the cosmological models on the anisotropy of UHECRs over the whole range of energy considered. This is because each model has a different set of model parameters due to which it provides a different effective Hubble parameter value from the others as mentioned earlier (see Fig. 1) and hence provides a different anisotropy value than the rest.

For the comparison of our findings with the results of available literature, we consider the results of Ref. [4] in which only Λ CDM model was taken into consideration. In this context, it needs to be mentioned that we consider the energy spectral index $\gamma = 2.7$ and coherence length $l_c = 0.25$ Mpc with a range of magnetic field values in our work. Whereas in Ref. [4] $\gamma = 2$ and $l_c = 1$ Mpc have been used. Thus for verifying our results with that of the Ref. [4], we calculate the dipolar anisotropy values of UHECRs within the corresponding energy range with $\gamma = 2$, $B = 1$ nG and $l_c = 1$ Mpc for the Λ CDM model only. The results

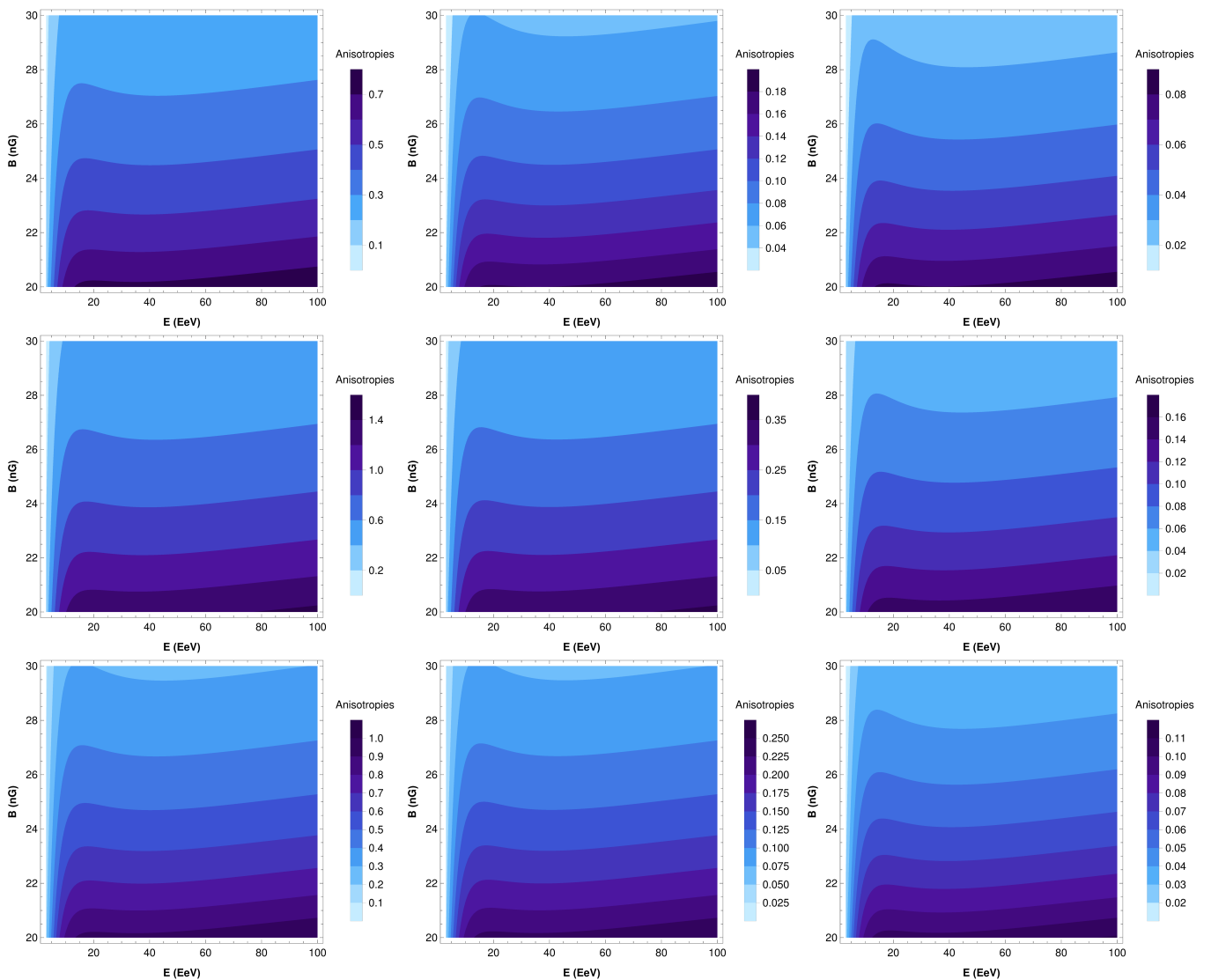


FIG. 2. Anisotropies of UHECRs for the Λ CDM model (top panels), $f(R)$ power-law model (middle panels) and the Starobinsky model (bottom panels) at selected source distances of 30, 60, and 90 Mpc (from left to right) for each of the models. Here for simplicity composition of CRs is considered as pure proton.

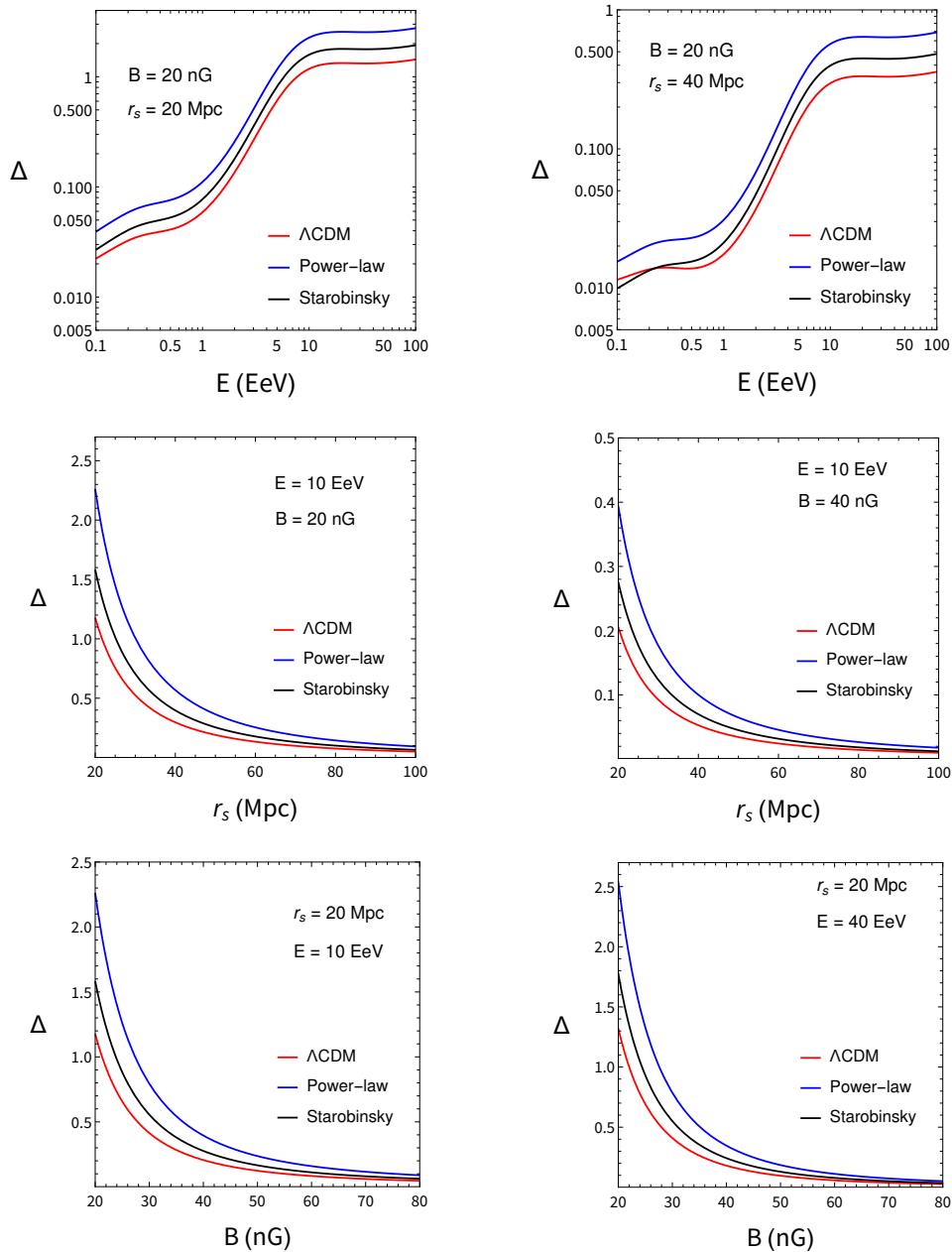


FIG. 3. Comparison of UHECRs' anisotropy as a function of energy (top panels), source distance (middle panels) and magnetic field strength (bottom panels) for different cosmological models.

are as shown in the right panel of Fig. 4 in comparison to that of Ref. [4] for two source distances of 25 Mpc and 50 Mpc. The dots shown in the plot are obtained from the integration of the stochastic differential equation as shown in Ref. [4], while the solid lines represent the anisotropy from our results and show a very good agreement.

Further, we draw the contour plots of UHECRs' anisotropy considering the nuclei as the UHECRs composition in Fig. 5. It is to be noted however that the formation of secondary nucleons during photo-disintegration processes affects nuclear masses, making it challenging to account for energy losses in the case of nuclei [4]. For such a nuclear composition, one has to replace E by E/Z , where Z is the atomic number. The anisotropy levels of these nuclei are quite different from the pure proton case. Here, we again consider the Λ CDM model, power-law model, and the Starobinsky model taking the source at a distance $r_s = 30$ Mpc. We consider He, C and Fe nuclei with a $E^{-2.7}$ spectral distribution by taking the energy range from 4 EeV upto $6Z$ EeV [102]. For instance, in the He nuclei case, the energy range is from 4 EeV to 12 EeV. We see that the anisotropy increases with increasing energy and decreasing magnetic field strength. In the case of the carbon nuclei, the variations of anisotropy are more quicker with energy and magnetic field, while for the iron nuclei, the lower value of anisotropy covers most of the range and

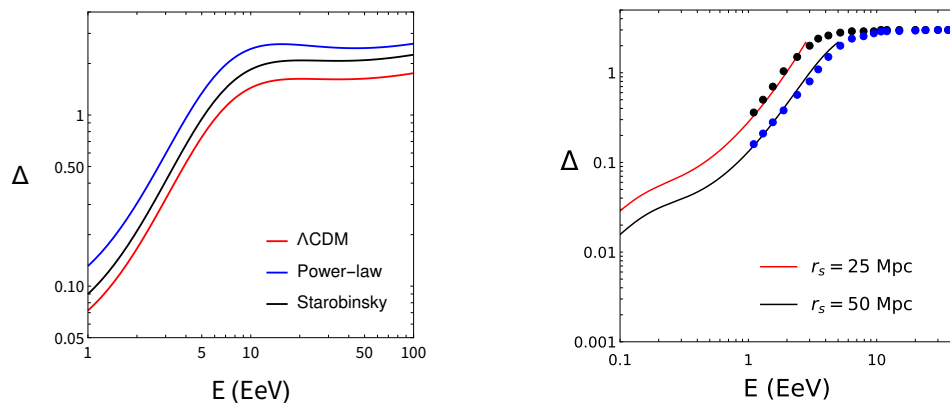


FIG. 4. Left: Variation of UHECRs' anisotropy with respect to the energy for the Λ CDM model, $f(R)$ power-law model and the Starobinsky model. Right: The anisotropy obtained for the Λ CDM model of this present work (solid lines) along with the results obtained from the stochastic differential equation as shown in Ref. [4]

also they have a rapid variation of anisotropy than the carbon nuclei. These behaviours of carbon and helium nuclei also have some dependency on the cosmological model considered. The small values of anisotropy and their behaviours in the case of considered nuclei may be due to the attribution of the process of photo-disintegration as mentioned above, for which heavier nuclei are likely to be more prone. Again, if we take a look at the cosmological models considered here, the power-law model depicts the highest value of anisotropy, while the Λ CDM model shows the lowest value. The Starobinsky model shows the results between the Λ CDM model and the power-law model. The higher anisotropy is obtained for lighter nuclei as compared to the heavier nuclei [102].

Finally, for a general picture of the effect of magnetic field on the anisotropy of UHECRs, we consider a scenario, where UHECRs propagate through a TMFs of 10 – 100 nG within a 1 Mpc thick plane. Fig. 6 shows the results of this scenario. We observed that the level of anisotropy is high for the low value of magnetic fields and low (< 0.2) for the high value of magnetic fields. The low-level anisotropy is almost the same for all three cosmological models. The low-level anisotropies dominate most of the range we considered. The effect of the cosmological model for low-value anisotropy is less as compared to the cases we have discussed earlier. These results are due to the fact that the small source distance and the strength of the magnetic fields dominate the effects on the anisotropy of UHECRs.

IV. SUMMARY AND CONCLUSION

In this study, we considered in detail the diffusion of charged particles in TMFs and calculated the dipolar anisotropies of CRs in the energy range from 0.1 EeV 100 EeV for the Λ CDM model, $f(R)$ power-law model and the Starobinsky model under the assumption of pure proton as well as pure helium, carbon and iron nuclei composition of UHECRs. We found that the anisotropy for the Λ CDM model and the Starobinsky model are almost identical to each other. On the other hand, the $f(R)$ power-law shows the highest anisotropy whether it is for protons and other nuclei. In the iron nuclei case, the lower range of dipolar amplitude dominated the plots in all those cosmological models considered here. To summarize the dependency of various factors such as energy, magnetic field, source distance, and also the cosmological model on the UHECRs anisotropy, we draw the slice contour plots in Fig. 7 by keeping a range of anisotropy for all these models from 0.4 to 0.5. From these plots, we can conclude that for the higher value of anisotropy, the required conditions are: higher energy, weak magnetic field strength, and closer to the source distance. These conditions are the results of the facts that high energetic CRs from a source at a particular distance are deflected less by a weak magnetic field than a strong magnetic field. Similarly, CRs from a nearby source with a particular energy have been deflected less by a magnetic field of a given strength than CRs from a distant source but with the same energy at the source. Thus, high energetic UHECRs from a nearby source in a weak magnetic field will be deflected very little from the source direction during their propagation, which leads to higher anisotropic distribution of UHECRs. For the same value of anisotropy with the given values of energy and magnetic field, the source distance depends on the cosmological model. For example, the anisotropy amplitude of 0.5 has been obtained (for certain values of magnetic field and energy) at source distances of ~ 37 Mpc and ~ 33 Mpc for the power-law model and the Starobinsky model respectively. While the same magnitude of anisotropy can be obtained at a source distance of ~ 30 Mpc in the Λ CDM model. Overall, the level of anisotropies of UHECRs predicted by our considered $f(R)$ gravity models which are in comparison to the prediction of the Λ CDM model are found to be consistent with observations at EeV energies [4, 76].

At this point, it is to be noted that as our nearby Universe (within 100 Mpc) does not have a uniform distribution of sources,

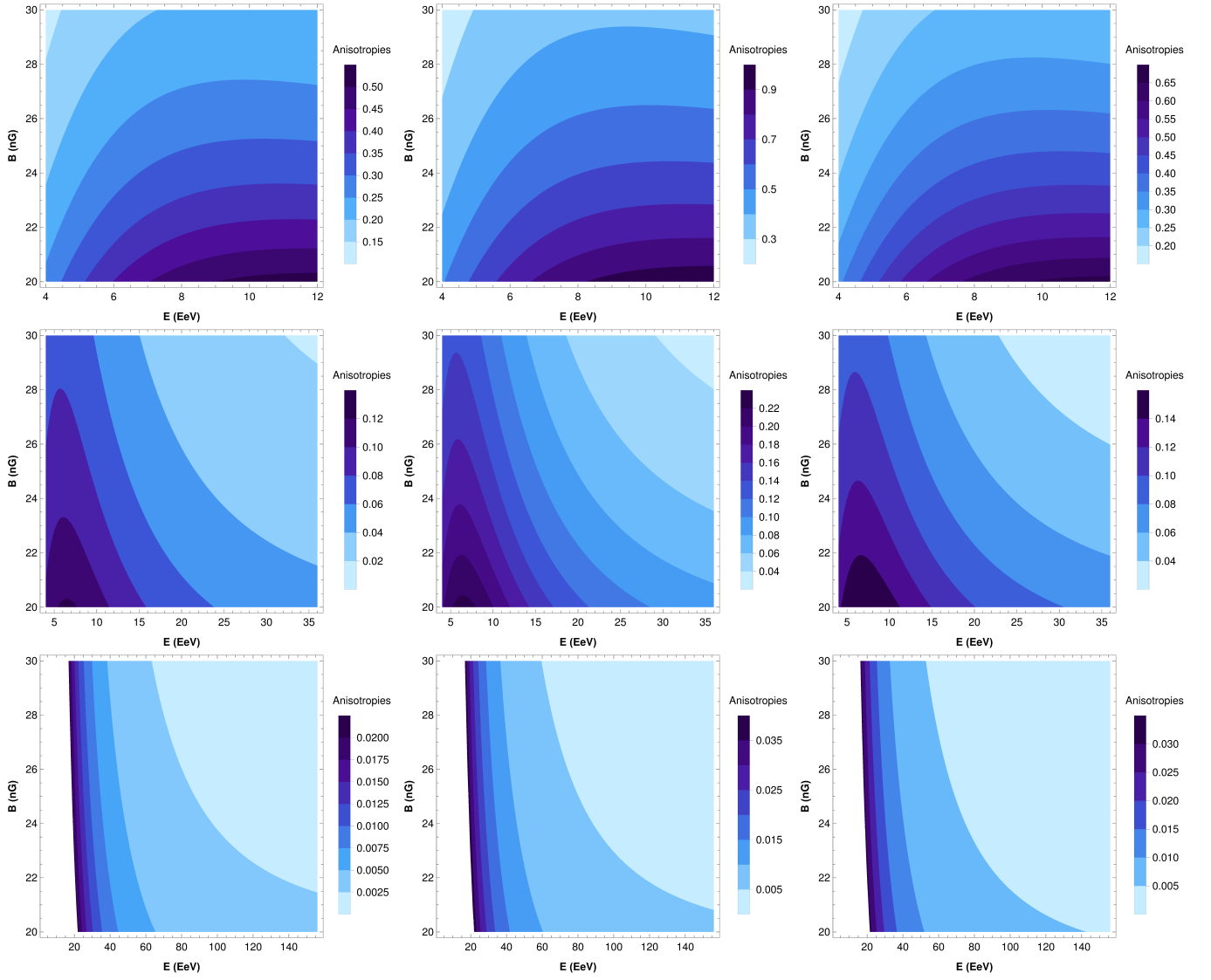


FIG. 5. UHECRs' anisotropy for pure helium (top panels), carbon (middle panels) and iron (bottom panels) nuclei for the Λ CDM model, $f(R)$ power-law model and the Starobinsky model (vertical panels from left to right) respectively at 30 Mpc source distance.

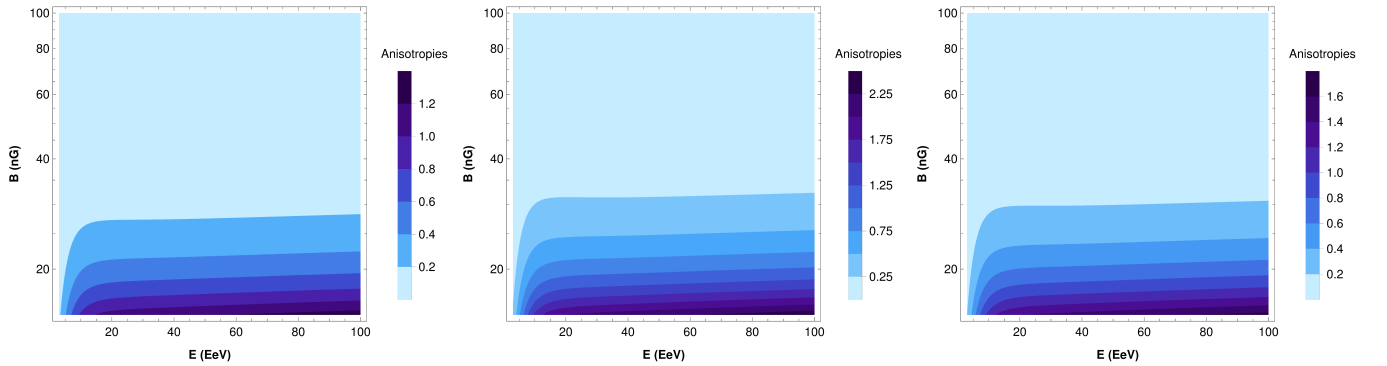


FIG. 6. Variation of UHECRs' anisotropy as a function of the energy and the wide range of magnetic field strengths within a 1 Mpc thick plane for the Λ CDM model (left panel), $f(R)$ power-law model (middle panel) and the Starobinsky model (right panel).

some directions have more sources than others. It is anticipated that, when this anisotropy is taken into account (for 2MRS

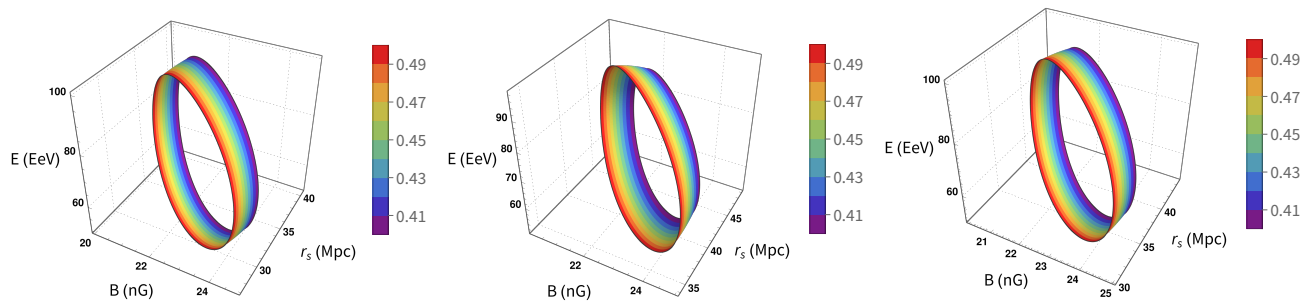


FIG. 7. Variation of UHECRs' anisotropy with respect to energy, magnetic field strength, and source distance according to the Λ CDM model, $f(R)$ power-law model and the Starobinsky model.

galaxy catalog), the CRs distribution's dipole amplitude will rise by a factor of 1.5 to 2 [4]. The CR distribution's asymmetry is indicated by this dipole amplitude, and as it grows, the CR distribution will become more lopsided. The direction of the dipole amplitude is also predicted to be the same as the direction of motion of the Local Group [4, 103], which is the galaxy cluster that we are a part of. In comparison to the anisotropies that the Compton-Getting effect would produce, the anisotropies in the CRs distribution that are brought about by the anisotropies in the galaxy distribution are substantially bigger [104]. Thus the anisotropy in the local distribution of sources is predicted to cause the anisotropy in CRs distribution.

It is important to note that additional deflections of CRs, primarily due to the galactic magnetic field, can alter both the amplitude and direction of the CR dipole. This can also lead to the creation of higher-order multipoles in the distribution of arrival directions [4]. For energies below a few EeV, these effects could potentially diminish the amplitudes calculated in this study to some degree.

As mentioned earlier, since the main aim of this work is to understand the possible effects of $f(R)$ gravity theory on the anisotropic distribution of UHECRs during their diffusive propagation process in TMFs, our results are not quantified in the sense of experimental data. However, the results of this work provide important information about the diffusion of UHECRs in the TMFs. The dipolar anisotropy observed in UHECRs provides a valuable window into the underlying cosmological and astrophysical processes governing their propagation. As future experiments will provide more precise data on UHECRs, our work may help to establish a framework for discerning the underlying cosmological model that best explains the observed dipolar anisotropy. In conclusion, our study advances the comprehension of UHECRs' dipolar anisotropy within the diffusive regime by examining its manifestation in the context of the Λ CDM model, the $f(R)$ power-law model, and the Starobinsky model. The diverse predictions offered by these models underscore the importance of refining our understanding of UHECRs' sources, propagation, and the fundamental nature of gravity through continued experimental observations and theoretical investigations. However, we made several assumptions for simplicity. We considered a single source of UHECRs at varying distances, which may not capture the complexity of multiple sources. The galactic magnetic field, which can significantly affect UHECRs' propagation, was not included in our model. We also assumed that UHECRs' propagate through turbulent magnetic fields in extragalactic space, without considering structured fields. These assumptions, while necessary for this study, could be relaxed in future work to provide a more comprehensive model of UHECRs' propagation and anisotropy.

The complexity of distinguishing the effects of different cosmological models on the anisotropy of UHECRs arises from several factors. The unknown sources of UHECRs and their distribution can introduce anisotropies that might be misattributed to the cosmological models. The strength and structure of the magnetic fields, which are not well known, can deflect UHECRs and cause anisotropies, making it challenging to separate these effects from those of the cosmological model. The composition of UHECRs, another source of uncertainty, can affect the observed anisotropy as different particles interact differently with the intergalactic magnetic fields and the cosmic microwave background. Despite these uncertainties, statistical methods and careful assumptions may allow us to estimate the relative contributions of these factors to the observed anisotropy, enabling us to infer the properties of the cosmological models, the magnetic fields, and the UHECR sources and compositions. Further observational data and theoretical developments will be crucial in refining these estimates and improving our understanding of UHECRs. This work can be extended by taking into consideration other MTGs as well as the multiple sources along with the experimental data for the quantified and realistic analysis to understand the anisotropies of UHECRs.

ACKNOWLEDGEMENTS

UDG is thankful to the Inter-University Centre for Astronomy and Astrophysics (IUCAA), Pune, India for awarding the Visiting Associateship of the institute.

-
- [1] P. Blasi, *The Origin of Galactic Cosmic Rays*, *Astron. Astrophys. Rev.* **21**, 70 (2013), [arXiv:1311.7346].
- [2] E. G. Berezhko, H. Volk, *Spectrum of cosmic rays, produced in supernova remnants*, *Astrophys. J. Lett.* **661**, L175 (2007) [arXiv:0704.1715].
- [3] J. W. Hewitt, M. Lemoine-Goumard, *Observations of supernova remnants and pulsar wind nebulae at gamma-ray energies*, *Comptes rendus Physique* **16**, 674 (2015).
- [4] D. Harari, S. Mollerach, E. Roulet, *Anisotropies of ultrahigh energy cosmic rays diffusing from extragalactic sources*, *Phys. Rev. D* **89**, 123001 (2014) [arXiv:1312.1366].
- [5] A. Aab et al. (Pierre Auger Collaboration), *Inferences on mass composition and tests of hadronic interactions from 0.3 to 100 EeV using the water-Cherenkov detectors of the Pierre Auger Observatory*, *Phys. Rev. D* **96**, 122003 (2017).
- [6] P. Abreu et al. (Pierre Auger Collaboration), *Constraints on the origin of cosmic rays above 10^{18} eV from large scale anisotropy searches in data of the Pierre Auger Observatory*, *Astrophys. J. Lett.* **762** (2013) L13 [arXiv:1212.3083v1].
- [7] R.U. Abbasi (Telescope Array Collaboration), *Search for EeV Protons of Galactic Origin*, *Astropart. Phys.* **86**, 21 (2017) [arXiv:1608.06306v2].
- [8] A. Aab et al. (Pierre Auger Collaboration), *Observation of a Large-scale Anisotropy in the Arrival Directions of Cosmic Rays above 8×10^{18} eV*, *Science* **357**, 1266 (2017) [arXiv:1709.07321v1].
- [9] A. M. Hillas, *The energy spectrum of cosmic rays in an evolving universe*, *Phys. Lett. A* **24**, 677 (1967).
- [10] G. R. Blumenthal, *Energy Loss of High-Energy Cosmic Rays in Pair-Producing Collisions with Ambient Photons*, *Phys. Rev. D* **1**, 1596 (1970).
- [11] V. Berezhinsky, A. Z. Gazizov, S. I. Grigorieva, *On astrophysical solution to ultrahigh energy cosmic rays*, *Phys. Rev. D* **74**, 043005 (2006) [arXiv:hep-ph/0204357].
- [12] M. Lemoine, *Extragalactic magnetic fields and the second knee in the cosmic-ray spectrum*, *Phys. Rev. D* **71**, 083007 (2005) [arXiv:astro-ph/0411173].
- [13] A. Aab et al. (The Pierre Auger Collaboration), *Features of the Energy Spectrum of Cosmic Rays above 2.5×10^{18} eV Using the Pierre Auger Observatory*, *Phys. Rev. Lett.* **125**, 121106 (2020) [arXiv:2008.06488].
- [14] A. Aab et al. (The Pierre Auger Collaboration), *Measurement of the cosmic-ray energy spectrum above 2.5×10^{18} eV using the Pierre Auger Observatory*, *Phys. Rev. D* **102**, 062005 (2020) [arXiv:2008.06486].
- [15] P. Abreu et al. (Pierre Auger Collaboration), *The energy spectrum of cosmic rays beyond the turn-down around 10^{17} eV as measured with the surface detector of the Pierre Auger Observatory*, *Eur. Phys. J. C* **81** (2021) 966 [arXiv:2109.13400v3].
- [16] V. Novotný, the Pierre Auger Collaboration, *Energy spectrum of cosmic rays measured using the Pierre Auger Observatory*, *PoS ICRC* **324** (2021).
- [17] R. U. Abbasi et al. (HiRes Collaboration), *First Observation of the Greisen-Zatsepin-Kuzmin Suppression*, *Phys. Rev. Lett.* **100** (2008) 101101 [arXiv:astro-ph/0703099v2].
- [18] J. Abraham et al. (The Pierre Auger Collaboration), *Observation of the Suppression of the Flux of Cosmic Rays above 4×10^{19} eV*, *Phys. Rev. Lett.* **101**, 061101 (2008) [arXiv:0806.4302v1].
- [19] T. Abu-Zayyad et al. (Telescope Array Collaboration), *The Cosmic-Ray Energy Spectrum Observed with the Surface Detector of the Telescope Array Experiment*, *Astrophys. J.* **768**, L1 (2013).
- [20] K. Greisen, *End to the Cosmic-Ray Spectrum?*, *Phys. Rev. Lett.* **16**, (1966) 748.
- [21] G.T. Zatsepin, V.A. Kuz'min, *Upper Limit of the Spectrum of Cosmic Rays*, *JETP Lett.* **4**, 78 (1966).
- [22] J. Abraham et al., (Pierre Auger Collaboration), *Upper limit on the cosmic-ray photon fraction at EeV energies from the Pierre Auger Observatory*, *Astropart. Phys.* **31**, 399 (2009) [arXiv:0903.1127v2].
- [23] T. Abu-Zayyad et al. (Telescope Array Collaboration), *Upper limit on the flux of photons with energies above 10^{19} eV using the Telescope Array surface detector*, *Phys. Rev. D* **88**, 112005 (2013) [arXiv:1304.5614].
- [24] P. Abreu et al. (Pierre Auger Collaboration), *Search for photons above 10^{19} eV with the surface detector of the Pierre Auger Observatory*, *JCAP* **05**, 021 (2023) [arXiv:2209.05926].
- [25] P. Abreu et al., (Pierre Auger Collaboration), *Search for Point-like Sources of Ultra-high Energy Neutrinos at the Pierre Auger Observatory and Improved Limit on the Diffuse Flux of Tau Neutrinos*, *Astrophys. J.* **755**, L4 (2012).
- [26] M. G. Aartsen et al., (IceCube Collaboration), *Search for a diffuse flux of astrophysical muon neutrinos with the IceCube 59-string configuration*, *Phys. Rev. D* **89**, 062007 (2014) [arXiv:1311.7048].
- [27] A. Aab et al. (Pierre Auger Collaboration), *Probing the origin of ultra-high-energy cosmic rays with neutrinos in the EeV energy range using the Pierre Auger Observatory*, *JCAP* **10**, 022 (2019) [arXiv:1906.07422].
- [28] P. Abreu et al., (Pierre Auger Collaboration), *A Search for Point Sources of EeV Neutrons*, *Astrophys. J.* **760**, 148 (2012).
- [29] J. Abraham et al., (Pierre Auger Collaboration), *Measurement of the Depth of Maximum of Extensive Air Showers above 10^{18} eV*, *Phys. Rev. Lett.* **104**, 091101 (2010) [arXiv:1002.0699v1].
- [30] Pierre Auger Collaboration, *Interpretation of the depths of maximum of extensive air showers measured by the Pierre Auger Observatory*, *JCAP* **02**, 026 (2013).

- [31] A. Aab et al. (Pierre Auger Collaboration), *Depth of maximum of air-shower profiles at the Pierre Auger Observatory. I. Measurements at energies above $10^{17.8}$ eV*, *Phys. Rev. D* **90**, 122005 (2014) [arXiv:1409.4809].
- [32] A. Aab et al. (Pierre Auger Collaboration), *Depth of maximum of air-shower profiles at the Pierre Auger Observatory. II. Composition implications*, *Phys. Rev. D* **90**, 122006 (2014) [arXiv:1409.5083].
- [33] S. Mollerach, E. Roulet, *Progress in high-energy cosmic ray physics*, *Prog. Part. Nucl. Phys.* **98**, 85 (2018) [arXiv:1710.11155].
- [34] O. Deligny, K. Kawata, P. Tinyakov, *Measurement of anisotropy and the search for ultra high energy cosmic ray sources*, *PTEP* **2017**, 12A104 (2017) [arXiv:1702.07209].
- [35] O. Deligny, *Measurements and implications of cosmic ray anisotropies from TeV to trans-EeV energies*, *Astropart. Phys.* **104**, 13 (2019) [arXiv:1808.03940].
- [36] A. Aab et al. (Pierre Auger Collaboration), *Large-scale Cosmic-Ray Anisotropies above 4 EeV Measured by the Pierre Auger Observatory*, *Astrophys. J.* **868**, 4 (2018) [arXiv:1808.03579].
- [37] P. Blasi and A. V. Olinto, *Magnetized local supercluster and the origin of the highest energy cosmic rays*, *Phys. Rev. D* **59**, 023001 (1999).
- [38] A. M. Taylor, M. Ahlers and F. A. Aharonian, *Need for a local source of ultrahigh-energy cosmic-ray nuclei*, *Phys. Rev. D* **84**, 105007 (2011).
- [39] J. H. Matthews, A.R. Bell, K.M. Blundell and A.T. Araudo, *Fornax A, Centaurus A, and other radio galaxies as sources of ultrahigh energy cosmic rays*, *MNRAS Lett.* **479**, L76 (2018).
- [40] R. Guedes Lang, A. M. Taylor, M. Ahlers and V. de Souza, *Revisiting the distance to the nearest ultrahigh energy cosmic ray source: Effects of extragalactic magnetic fields*, *Phys. Rev. D* **102** 063012 (2020).
- [41] A. Aab et al., (Pierre Auger Collaboration), *Cosmic-Ray Anisotropies in Right Ascension Measured by the Pierre Auger Observatory*, *Astrophys. J.* **891**, 142 (2020) [arXiv:2002.06172].
- [42] P. Abeu et al., *Arrival Directions of Cosmic Rays above 32 EeV from Phase One of the Pierre Auger Observatory*, *Astrophys. J.* **935**, 170 (2022) [arXiv:2206.13492].
- [43] A. Aab. et al., (Pierre Auger Collaboration), *Indication of anisotropy in arrival directions of ultra-high-energy cosmic rays through comparison to the flux pattern of extragalactic gamma-ray sources*, *Astrophys. J. Lett.*, **853**:L29 (2018) [arXiv:1801.06160]
- [44] R. U. Abbasi et al.,(Telescope Array Collaboration), *Search for Large-scale Anisotropy on Arrival Directions of Ultra-high-energy Cosmic Rays Observed with the Telescope Array Experiment*, *Astrophys. J. Lett.* **898**, L28 (2020) [arXiv:2007.00023].
- [45] R. U. Abbasi et al.,(Telescope Array Collaboration), *Evidence of Intermediate-scale Energy Spectrum Anisotropy of Cosmic Rays $E \geq 10^{19.2}$ eV with the Telescope Array Surface Detector*, *Astrophys. J.* **862**, 91 (2018).
- [46] R. U. Abbasi et al.,(Telescope Array Collaboration), *Indications of a Cosmic Ray Source in the Perseus-Pisces Supercluster*, [arXiv:2110.14827].
- [47] P. Tinyakov et al., (Telescope Array Collaboration), *The UHECR dipole and quadrupole in the latest data from the original Auger and TA surface detectors*, *PoS ICRC*, **375** (2021)]
- [48] B. P. Abbott et al. (LIGO Scientific Collaboration and Virgo Collaboration), *Observation of Gravitational Waves from a Binary Black Hole Merger*, *Phys. Rev. Lett.* **116**, 061102 (2016) [arXiv:1602.03837].
- [49] The Event Horizon Telescope Collaboration et al., *First M87 Event Horizon Telescope Results. I. The Shadow of the Supermassive Black Hole*, *Astrophys. J. Lett.* **871**, L1 (2019).
- [50] The Event Horizon Telescope Collaboration et al., *First M87 Event Horizon Telescope Results. II. Array and Instrumentation*, *Astrophys. J. Lett.* **875**, L2 (2019).
- [51] The Event Horizon Telescope Collaboration et al., *First M87 Event Horizon Telescope Results. III. Data Processing and Calibration*, *Astrophys. J. Lett.* **875**, L3 (2019).
- [52] The Event Horizon Telescope Collaboration et al., *First M87 Event Horizon Telescope Results. IV. Imaging the Central Supermassive Black Hole*, *Astrophys. J. Lett.* **875**, L4 (2019).
- [53] The Event Horizon Telescope Collaboration et al., *First M87 Event Horizon Telescope Results. V. Physical Origin of the Asymmetric Ring*, *Astrophys. J. Lett.* **875**, L5 (2019).
- [54] The Event Horizon Telescope Collaboration et al., *First M87 Event Horizon Telescope Results. VI. The Shadow and Mass of the Central Black Hole*, *Astrophys. J. Lett.* **875**, L6 (2019).
- [55] A. G. Reiss et al., *Observational Evidence from Supernovae for an Accelerating Universe and a Cosmological Constant*, *Astron. J.* **116**, 1009 (1998) [arXiv:astro-ph/9805201].
- [56] S. Perlmutter et al., *Measurements of Ω and Λ from 42 High-Redshift Supernovae*, *Astrophys. J.* **517**, 565 (1999) [arXiv:astro-ph/9812133].
- [57] D. N. Spergel et al., *Three-Year Wilkinson Microwave Anisotropy Probe (WMAP) Observations: Implications for Cosmology*, *Astrophys. J. Suppl. S* **170**, 377 (2007) [arXiv:astro-ph/0603449].
- [58] P. Astier et al., *The Supernova Legacy Survey: Measurement of Ω_M , Ω_Λ and ω from the First Year Data Set*, *A & A* **447**, 31 (2006) [arXiv:astro-ph/0510447].
- [59] J. H. Oort, *The force exerted by the stellar system in the direction perpendicular to the galactic plane and some related problems*, *Bull. Astron. Inst. the Netherlands.* **6**, 249 (1932).
- [60] F. Zwicky, *Helv. Phys. Acta.* **6**, 110-127 (1933); F. Zwicky, *Republication of: The redshift of extragalactic nebulae*, *Gen. Relativ. Gravit.* **41**, 207224 (2009).
- [61] F. Zwicky, *On the Masses of Nebulae and of Clusters of Nebulae*, *Astrophys. J.* **86**, 217-246 (1937).
- [62] K. Garrett and G. Duda, *Dark Matter: A Primer*, *Adv. Astron.*, 968283 (2011) [arXiv:1006.2483].
- [63] N. Parbin, U. D. Goswami, *Galactic rotation dynamics in a new $f(R)$ gravity model*, *Eur. Phys. J. C* **83**, 411 (2023) [arXiv:2208.06564].
- [64] E. J. Copeland, M. Sami, S. Tsujikawa, *Dynamics of dark energy*, *IJMP D* **15**, 1753-1936 (2006) [arXiv:hep-th/0603057].

- [65] U. D. Goswami, H. Nandan, M. Sami, *Formation of caustics in Dirac-Born-Infeld type scalar field systems*, *Phys. Rev. D* **82**, 103530 (2010).
- [66] P. Sotiriou, V. Faraoni, *$f(R)$ theories of gravity*, *Rev. Mod. Phys.* **82**, 451 (2010) [arXiv:0805.1726].
- [67] A. A. Starobinsky, *Disappearing cosmological constant in $f(R)$ gravity*, *JETP. Lett.* **86**, 157 (2007) [arXiv:0706.2041].
- [68] A. A. Starobinsky, *A New Type of Isotropic Cosmological Models without Singularity*, *Phys. Lett. B* **91**, 99 (1980).
- [69] W. Hu and I. Sawicki, *Models of $f(R)$ cosmic acceleration that evade solar system tests*, *Phys. Rev. D* **76**, 064004 (2007) [arXiv:0705.1158v1].
- [70] D. J. Gogoi, U. D. Goswami, *Cosmology with a new $f(R)$ gravity model in Palatini formalism*, *IJMP D* **31**, 2250048 (2022) [arXiv:2108.01409].
- [71] U. D. Goswami, K. Deka, *Cosmological Dynamics of $f(R)$ Gravity Scalar Degree of Freedom in Einstein Frame*, *IJMP D* **22**, 13 (2013) 1350083 [arXiv:1303.5868].
- [72] S. Tsujikawa, *Observational signatures of $f(R)$ dark energy models that satisfy cosmological and local gravity constraints*, *Phys. Rev. D* **77**, 023507 (2008) [arXiv:0709.1391v2].
- [73] P. Mertsch, M. Ahlers, *Cosmic Ray Small-Scale Anisotropies in Quasi-Linear Theory*, *JCAP* **11**, 048 (2019) [arXiv:1909.09052v2].
- [74] S. Mollerach, E. Roulet, *Ultra-high energy cosmic rays from a nearby extragalactic source in the diffusive regime*, *Phys. Rev. D* **99**, 103010 (2019) [arXiv:1903.05722].
- [75] S. Mollerach, E. Roulet, *Anisotropies of ultra-high-energy cosmic rays in a scenario with nearby sources*, *Phys. Rev. D* **105**, 063001 (2022) [arXiv:2111.00560v2].
- [76] D. Harari, S. Mollerach, E. Roulet, *Cosmic ray anisotropies from transient extragalactic sources*, *Phys. Rev. D* **103**, 023012 (2021) [arXiv:2010.10629v2].
- [77] M. Ahlers, P. Mertsch, *Origin of Small-Scale Anisotropies in Galactic Cosmic Rays*, *Prog. Part. Nucl. Phys.* **94**, 184 (2017) [arXiv:1612.01873v1].
- [78] S. Mollerach, E. Roulet, O. Taborada, *Large-scale anisotropies of extragalactic cosmic rays below the ankle*, *JCAP* **12**, 021 (2022) [arXiv:2207.11540v2].
- [79] A. U. Abeysekara et al., *All-sky Measurement of the Anisotropy of Cosmic Rays at 10 TeV and Mapping of the Local Interstellar Magnetic Field*, *Astrophys. J* **871**, 96 (2019).
- [80] M. Chakraborty et al., (Grapes-3 Collaboration), *Large-scale cosmic ray anisotropy measured by the GRAPES-3 experiment*, *PoS ICRC* **395** (2021).
- [81] N. Globus et al., *Cosmic ray anisotropy from large-scale structure and the effect of magnetic horizons*, *MNRAS* **484**, 4167 (2019).
- [82] G. Sigl, M. Lemoine, P. Biermann, *Ultra-High Energy Cosmic Ray Propagation in the Local Supercluster* *Astropart. Phys.* **10** (1999) 141
- [83] P. Sarmah, A. De, U. D. Goswami, *Anisotropic LRS-BI Universe with $f(Q)$ gravity theory*, *Phys. Dark Universe* **40**, 101209 (2023) [arXiv:2303.05905].
- [84] D. J. Gogoi and U. D. Goswami, *A new $f(R)$ Gravity Model and properties of Gravitational Waves in it*, *Eur. Phys. J. C* **80**, 1101 (2020) [arXiv:2006.04011].
- [85] J. Bora, D. J. Gogoi, U. D. Goswami, *Strange stars in $f(R)$ gravity Palatini formalism and gravitational wave echoes from them*, *JCAP* **09**, 057 (2022) [arXiv:2204.05473v2].
- [86] N. Parbin, D. J. Gogoi, U. D. Goswami, *Weak gravitational lensing and shadow cast by rotating black holes in axionic Chern-Simons theory*, *Phys. Dark Universe* **41**, 101265 (2023) [arXiv:2305.09157].
- [87] R. Karmakar, D. J. Gogoi, U. D. Goswami, *Thermodynamics and shadows of GUP-corrected black holes with topological defects in Bumblebee gravity*, *Phys. Dark Universe* **41**, 101249 (2023) [arXiv:2303.00297].
- [88] N. Parbin et al., *Deflection angle, quasinormal modes and optical properties of a de Sitter black hole in $f(T, B)$ gravity*, *Phys. Dark Universe* **42**, 101315 (2023) [arXiv:2211.02414].
- [89] S. P. Sarmah, U. D. Goswami, *Propagation and Fluxes of Ultra High Energy Cosmic Rays in $f(R)$ Gravity Theory*, *Eur. Phys. J. C* **84**, 419 (2024) [arXiv:2303.16678].
- [90] N. Aghanim et al., *Planck 2018 results* (Planck Collaboration), *A & A* **641**, A6 (2020) [arXiv:1807.06209].
- [91] K. Nakamura and Particle Data Group, *Review of Particle Physics*, *J. Phys. G: Nucl. Part. Phys.* **37**, 075021(2010).
- [92] Y. Hu et al., *Turbulent Magnetic Field Amplification by the Interaction of a Shock Wave and Inhomogeneous Medium*, *Astrophys. J.* **941**, 133 (2022).
- [93] U. Chadayammuri, *Turbulent magnetic fields in merging clusters: a case study of Abell 2146*, *MNRAS* **512**, 2 (2022).
- [94] L. Feretti et al., *Clusters of galaxies: observational properties of the diffuse radio emission*, *Astron. Astrophys. Rev.* **20**, 54 (2012).
- [95] J. P. Vallée, *A Synthesis of Fundamental Parameters of Spiral Arms, Based on Recent Observations in the Milky Way*, *New Astro. Rev.* **55**, 91 (2011).
- [96] F. Vazza et al., *Simulations of extragalactic magnetic fields and of their observables*, *Class. Quantum Grav.* **34**, 234001 (2017).
- [97] G. Sigl, F. Miniati and T. A. Ensslin, *Ultra-high energy cosmic ray probes of large scale structure and magnetic fields*, *Phys. Rev. D* **70**, 043007 (2004) [arXiv:astro-ph/0401084].
- [98] V. Berezhinsky, A. Z. Gazizov, *Diffusion of Cosmic Rays in the Expanding Universe. I.*, *Astrophys. J.* **643**, 8 (2006) [arXiv:astro-ph/0512090].
- [99] S. Mollerach, E. Roulet, *Magnetic diffusion effects on the Ultra-High Energy Cosmic Ray spectrum and composition*, *JCAP* **10**, 013 (2013) [arXiv:1305.6519].
- [100] S. I. Syrovatskii, *The Distribution of Relativistic Electrons in the Galaxy and the Spectrum of Synchrotron Radio Emission*, *Soviet Astro.* **3**, 22 (1959).
- [101] A. D. Supanitsky, *Cosmic ray propagation in the Universe in presence of a random magnetic field*, *JCAP* **04**, 046 (2021) [arXiv:2007.09063v2].

- [102] D. Harari, S. Mollerach, E. Roulet, *Anisotropies of ultra-high energy cosmic ray nuclei diffusing from extragalactic sources*, *Phys. Rev. D* **92**, 063014 (2015) [[arXiv:1507.06585](#)].
- [103] P. Erdogdu et al., *The dipole anisotropy of the 2 Micron All-Sky Redshift Survey*, *MNRAS* **368**, 1515 (2006).
- [104] M. Kachelriess, P. Serpico, *The Compton–Getting effect on ultra-high energy cosmic rays of cosmological origin*, *Phys. Lett. B* **640**, 225 (2006).